Article

Characteristics and Sources of CBM Well-Produced Water in the Shouyang Block, China

Bing Zhang [1,2], Gang Wang [3] , Wei Li [1,*] and Xinglong Jiao [1]

[1] Key Laboratory of Coalbed Methane Resources and Reservoir Formation Process, Ministry of Education, China University of Mining and Technology, Xuzhou 221008, China

[2] China United Coalbed Methane Corporation Ltd., Beijing 100011, China

[3] College of Architecture & Civil Engineering, Shangqiu Normal University, Shangqiu 476000, China

* Correspondence: kuangpuliwei@cumt.edu.cn

Abstract: The Shouyang Block was selected as the research subject. Comprehensive analysis was conducted using coalbed methane (CBM) well production data, geochemical test data on water produced from the coalbed methane well, and fundamental geological information. The findings reveal the water dynamics in the Shouyang Block are characterized by weak groundwater runoff or retention in most areas. The groundwater head height exhibits a gradual decrease from the north to south, which is closely associated with the monoclinic structure of the Shouyang Block. Overall, water production is relatively high. As the average water production increases, the average gas production gradually decreases. A concentration of high water production wells is observed in the northern part of the Shouyang Block, which gradually increases towards the southeast direction. A comprehensive analysis was conducted on the factors influencing water production, including total water content of coal seams, coal seam porosity, groundwater stability index, groundwater sealing coefficient, *D* value of the fracture fractal dimension, fault fractal dimension, and sand–mud ratio. The correlation degree was calculated and ranked in order of magnitude through grey correlation analysis. The order of factors that influence water production, from strongest to weakest, is as follows: sand–mud ratio > porosity > fractal dimension of fault > fracture fractal dimension *D* value > groundwater sealing coefficient > groundwater stability index > total water content of coal seams. The dissolution amounts of carbonate and sulfate are both small, and the water source may mainly come from the sandstone aquifer. Attention should be paid to the distribution and lithological combination of sandstone aquifers in coal-bearing strata in the future exploration and development process of the Shouyang Block. This will help to avoid the potential influence of fault structures and enable the identification of favorable areas for low water and high gas production.

Keywords: water production; influencing factors; coalbed methane well; China

1. Introduction

The extraction of coalbed methane is crucial for reducing methane emissions and ensuring safe production in coal mines, making it an essential unconventional clean energy source [1–5]. The production of coalbed methane is influenced by various geological factors, with hydrogeological conditions being particularly significant [6,7]. The changes in groundwater dynamic field can alter fluid pressure and flow direction, leading to changes in the direction and velocity of coalbed methane transport [7]. Groundwater flow can carry coalbed methane transport, resulting in higher gas content in areas with weak groundwater runoff and retention, and the formation of enriched coalbed methane reservoirs [6]. Groundwater chemical indicators, such as pH value, TDS, anion and cation concentration, trace element concentration, and hydrogen and oxygen isotopes can reflect dynamic characteristics of groundwater, and provide guidance for the exploration and development of coalbed methane [6–11]. In areas with weak runoff and stagnant flow, the

TDS is relatively high. As hydrodynamic forces weaken, the sodium chloride coefficient and carbonate equilibrium coefficient decrease from large to small [12].

However, groundwater is often supplied by external water sources, which coupled with the influence of structural factors such as faults and collapse columns, as well as fracturing factors, results in higher water production from coalbed methane wells [13]. The discharge of water affects the depressurization effect of the reservoir and the desorption of coalbed methane [11,14–16], which often results in high water production but low gas production [17]. Therefore, studying the characteristics and influencing factors of water production from coalbed methane wells is of great importance to further optimize coalbed methane development plans and increase gas production.

The Shouyang Block has abundant coal resources and high coalbed methane content. In the Taiyuan Formation, the gas content of No. 15 coal varies between 5.64 and 20.54 m^3/t, with a coalbed methane resource of 800×10^8 m^3 above [18]. However, No. 15 coal is mainly composed of anthracite, which belongs to the medium-to-high rank coal. The burial depth of coal seams is relatively deep, with low permeability, reservoir pressure, and gas saturation [12,18]. There is a sandstone aquifer in the upper part, resulting in high water production. The aforementioned factors have become important constraints in unlocking the production potential of coalbed methane wells [19]. Zhang Bing [20] used drilling, logging, drainage, and extraction data of coalbed methane wells to finely classify the thin layers of the Taiyuan Formation in coal-bearing aquifers. The limestone has limited impact on coalbed methane extraction due to its dense lithology, and low or no water content. The water-bearing sandstone layer above K_2 may be the main aquifer.

Previous studies on the water production of coalbed methane wells in the Shouyang Block often did not consider comprehensive factors, and the analysis was mostly qualitative. This article utilizes coalbed methane well discharge data, test data from coalbed methane well discharge water, and basic geological information to comprehensively analyze the groundwater dynamic field and hydrochemical parameters, as well as the various influencing factors of water production from the coalbed methane well. Reasons and models for high water production were examined. This analysis provides a theoretical basis for predicting favorable areas for "water avoidance and gas extraction" in the Shouyang Block.

The structure of the article is arranged in this way. Section 2 is the basic geological background, Section 3 is the methods, Section 4 is the analysis and discussion, and Section 5 is the conclusion.

2. Geological Background

2.1. Structural Geology

The Shouyang Block, covering an area of around 1718 km^2, is located at the northern Qinshui Basin, China [21]. Its structural composition primarily comprises a monocline that tilts towards the east–west and southward. Additionally, it features several secondary folds and faults (Figure 1).

2.2. Coal-Bearing Strata and Aquifers

The Taiyuan Formation and the Shanxi Formation comprise the primary coal-bearing strata in the Shouyang Block. The primary minable coal seam is the No. 15 coal, characterized by an average thickness of 2.8 m and average gas content of 12.97 m^3/t [22]. Consequently, No. 15 coal serves as the primary coalbed methane development seam at present.

The K_1 sandstone aquifer at the bottom of the Taiyuan Formation is partially in contact with the No. 15 coal, and is the principal aquifer situated beneath it. Within the Taiyuan Formation's upper and middle sections, three limestone layers can be found, namely K_2, K_3, and K_4. Certain regions have developed karst fissures and exhibit a high water content, which could potentially affect the drainage of the No. 15 coal. The thickness of the sandstone lens developed above the No. 15 coal varies significantly. This layer significantly

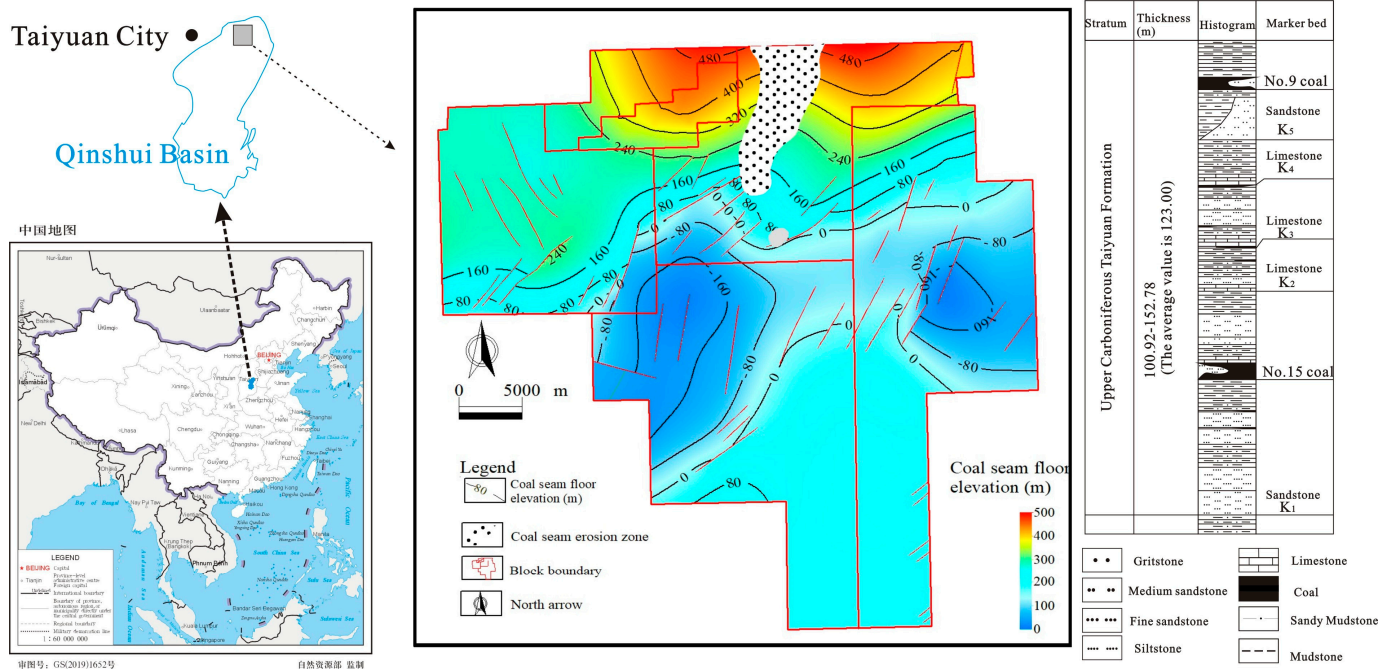influences water production, as it serves as the primary aquifer above the No. 15 coal seam (Figure 1).

Figure 1. Structural outline and stratigraphic distribution map of Shouyang Block. (Map of China cited from the website of the Ministry of Natural Resources of People's Republic of China).

3. Methodology

In the Shouyang Block, most of the coalbed methane wells mine a single layer of No. 15 coal, while others mine No. 3 + 15 coal and No. 3 + 9 + 15 coal. The research object of this study is the water discharged from the coalbed methane well during the mining of a single layer of No. 15 coal. Water samples were collected at the coalbed methane wellbore and subjected to anion and cation analysis, as well as hydrogen and oxygen isotope analysis.

Based on the dynamic liquid level depth (m) of the Shouyang Block's coalbed methane wells at the start of drainage, with 0 elevation as the reference plane, the total water head of various wells was determined. The resulting information was then used to create a distribution map showing the height of the water head across the Shouyang Block. The total water head was calculated according to the following equation:

$$h = z + h_{\mathrm{w}} \tag{1}$$

In the equation, h represents the total head (m). z stands for the elevation in the middle of the target layer (location head, m). h_{w} represents the height of the liquid column at the beginning of the drainage (equivalent to the piezometric head in the midpoint of the target layer, m), obtained by deducting the initial static liquid level depth (m) from the difference in elevation (m) between the wellhead altitude and the middle of the target layer.

The constant cation was determined by inductively coupled plasma spectrometry, with instrument model iCAP-7400, following the specifications and standards referenced in the "Chinese Environmental Protection Standard HJ 776-2015" of China [23]. HCO_3^- and CO_3^{2-} were determined by a titration method, following the specifications and standards referenced in "DZ/T 0064.49-2021" of China [24]. Cl^- was determined by a titration method, following the specifications and standards referenced in "DZ/T 0064.50-2021" of China [25]. SO_4^{2-} was determined by a gravimetric method, following the specifications and standards referenced in "GB/T 11899-1989" of China [26], while mineralization was

determined by a gravimetric method, following the specifications and standards referenced in "Methods for the Determination of Water and Wastewater" (Fourth Edition, Supplement). All experiments were conducted at the Jiangsu Institute of Geological and Mineral Resources Design and Research for testing. δ^2H and $\delta^{18}O$ isotope samples were sent to the Hydrochemistry Laboratory of the School of Resources and Geosciences, China University of Mining and Technology, for analysis and testing. The instrument used for testing was a stable isotope ratio mass spectrometer, model MAT253-EA, following the specifications referenced in "GB/T 37847-2019" of China [27]. The δ^2H and $\delta^{18}O$ values are calculated relative to the Vienna Standard Mean Ocean Water (VSMOW).

4. Results and Discussion

4.1. Characteristics of Discharge Water

4.1.1. Water Production

The average water production varies between 0.81 and 81.60 m^3/d, with an average of 10.69 m^3/d. Overall, water production is relatively high. A concentration of high water production wells is observed in the northern part of the Shouyang Block, which gradually increases towards the southeast direction (Figure 2). The average gas production varies between 0 and 760.57 m^3/d, with an average of 135.94 m^3/d. Overall, the gas production is relatively low. As the average water production increases, the average gas production gradually decreases. Excessive water production inhibits gas production efficiency [28]. When the average water production is less than 20 m^3/d, the average gas production undergoes significant changes, revealing an intimate relationship between gas production and water production in the Shouyang Block (Table 1; Figure 3).

Table 1. Average water production and average gas production data.

Well	W (m^3/d)	G (m^3/d)	Well	W (m^3/d)	G (m^3/d)
SY01	1.64	259.97	SY22	23.83	56.11
SY02	5.68	29.23	SY23	5.33	105.53
SY03	7.02	170.69	SY24	0.81	166.96
SY04	3.76	604.34	SY25	11.78	71.81
SY05	20.36	375.06	SY26	2.57	47.06
SY06	6.15	37.00	SY27	6.90	0.00
SY07	1.98	243.16	SY28	3.94	66.73
SY08	5.01	132.15	SY29	0.87	63.31
SY09	15.35	50.36	SY30	10.26	107.68
SY10	1.74	61.17	SY31	0.83	103.25
SY11	1.22	521.74	SY32	12.29	24.01
SY12	3.52	171.15	SY33	4.97	23.98
SY13	10.89	162.59	SY34	8.73	0.00
SY14	5.45	221.48	SY35	6.98	0.00
SY15	2.62	51.17	SY36	3.82	0.00
SY16	4.63	197.10	SY37	27.00	0.00
SY17	36.85	760.57	SY38	2.30	298.84
SY18	35.05	112.62	SY39	6.70	94.55
SY19	46.21	10.51	SY40	81.60	4.80
SY20	4.11	102.32	SY41	2.40	13.03
SY21	2.59	144.91	SY42	3.30	42.71

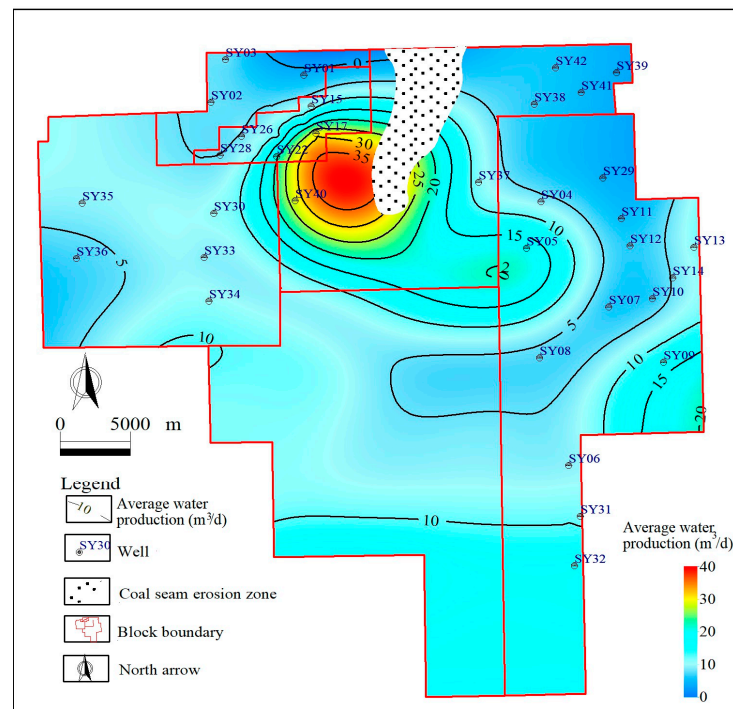*W*: average water production; *G*: average gas production.

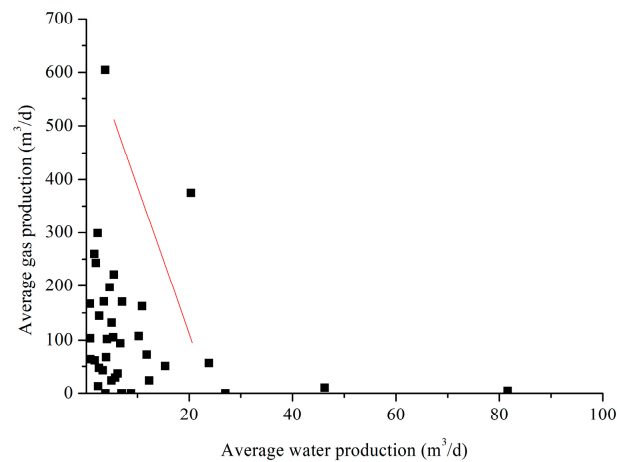**Figure 2.** Contour map of average water production of No. 15 coal.

Figure 3. Correlation of average water production with average gas production.

4.1.2. Hydrochemical Parameters

A total of 42 production wells in the research area were sampled for water analysis. The anion and cation concentrations were analyzed, and relevant parameters were calculated. (Table 2). TDS, sodium chloride coefficient, desulfurization coefficient, etc. are typical hydrochemical parameters used to reflect the characteristics of the groundwater environment. Upon analysis, it was discovered that the dominant ions in water are Na^+, Cl^-, and HCO_3^- with relatively high concentrations, indicating a Na-HCO_3 water type. The TDS of the water sample varies between 970.00 and 5334.00 mg/L, with an average of 2156.81 mg/L. The sodium chloride coefficient (rNa^+/rCl^-) of the water sample ranges from 0.16 to 6.85, with an average of 2.92; the desulfurization coefficient ($rSO_4^{2-} \times 100/rCl^-$) ranges from 0.12 to 13.75, with an average of 2.03. According to Wang et al. [7], groundwater with a sodium chloride coefficient lower than 10, a desulfurization coefficient lower than 1, and a TDS exceeding 1500 mg/L indicates a reducing environment with

weak groundwater activity [11,29]. Finally, the water dynamics in the Shouyang Block are characterized by weak groundwater runoff or retention in most areas.

Table 2. Ion concentrations of discharged water from coalbed methane wells.

Water Sample	Ca^{2+}	Mg^{2+}	$Na^+ + K^+$	HCO_3^-	CO_3^{2-}	SO_4^{2-}	Cl^-	TDS	$\delta^{18}O$ (‰)	δ^2H (‰)	Sealing Coefficient
				(mg/L)							
SW1	3.03	0.82	492.03	970.53	51.24	2.47	136.78	1102	-	-	261.17
SW2	4.79	4.23	1164.79	759.41	114.68	4.12	1104.01	2802	-	-	239.18
SW3	7.75	2.42	843.75	1230.49	71.29	4.12	561.78	2042	-	-	189.45
SW4	7.40	1.81	733.40	937.44	74.39	3.91	571.55	1802	-	-	176.58
SW5	18.20	4.97	874.20	1098.15	12.40	3.29	884.19	2414	-	-	108.43
SW6	4.57	1.58	713.57	978.41	77.49	2.88	500.71	1762	-	-	251.40
SW7	5.33	1.61	603.90	841.34	63.54	4.74	376.15	2798	-	-	161.38
SW8	9.06	2.73	756.70	721.60	37.19	4.12	679.02	2336	-	-	137.93
SW9	11.50	4.08	872.50	1143.84	26.35	3.70	720.54	2190	-	-	143.32
SW10	2.76	0.69	479.76	951.62	49.59	4.94	107.47	1088	-	-	189.33
SW11	20.10	5.36	975.10	918.54	38.74	3.29	975.78	2450	-	-	101.15
SW12	20.60	6.77	1180.60	697.96	49.59	2.88	1646.25	5334	-	-	118.16
SW13	28.00	8.03	1878.00	876.00	46.49	4.12	2557.30	5001	-	-	133.44
SW14	7.57	2.74	636.57	1124.94	55.02	2.47	297.99	1526	-	-	165.46
SW15	4.09	1.48	720.09	926.42	80.59	2.88	493.39	1688	-	-	262.78
SW16	18.10	5.17	1158.10	1233.65	38.74	4.53	1130.88	2914	-	-	128.11
SW17	22.40	6.19	1352.40	737.35	40.29	4.94	1675.56	1086	-	-	113.50
SW18	13.10	3.93	983.10	1131.24	30.99	5.35	847.55	1952	-	-	133.73
SW19	27.60	8.69	1067.60	1060.34	26.35	3.70	1187.06	3744	-	-	83.55
SW20	1.83	0.63	445.98	721.60	58.89	1.65	185.63	3496	-	-	343.58
SW21	1.89	0.80	411.88	705.84	41.84	1.65	158.76	3170	-	-	303.76
SW22	1.82	0.50	502.37	885.45	77.49	3.29	188.07	1124	−9.71	−72.7	294.72
SW23	1.56	0.53	503.92	833.46	82.13	3.50	185.63	1086	-	-	287.14
SW24	1.61	0.60	469.05	811.40	99.18	2.47	152.66	1020	−10.05	−74.92	327.41
SW25	3.20	1.23	656.90	825.59	67.42	6.59	434.77	1474	−8.85	−69.73	180.10
SW26	3.47	1.40	721.80	682.21	69.74	7.00	630.17	1732	-	-	177.25
SW27	1.88	0.66	544.95	915.39	111.58	11.11	185.63	1228	−9.35	−71.89	128.76
SW28	2.41	0.68	988.90	839.76	49.59	6.17	224.71	1110			227.10
SW29	2.22	0.64	438.77	819.28	55.79	1.65	124.57	970	−10.34	−75.96	318.94
SW30	2.12	0.53	476.24	849.21	75.94	2.68	144.11	1050	−9.71	−73.13	289.96
SW31	3.51	2.24	1144.00	735.49	78.49	37.04	1232.20	3235	-	-	74.55
SW32	3.69	2.60	735.56	644.27	67.30	47.75	663.54	2168	-	-	39.06
SW33	2.93	1.26	498.00	743.00	39.00	20.98	269.68	1591	-	-	61.58
SW34	4.31	2.18	655.00	701.00	81.30	23.68	491.49	1968	-	-	63.92
SW35	4.18	1.91	691.00	807.00	86.50	27.08	473.40	2100	-	-	62.03
SW36	2.27	0.84	549.50	1117.00	93.10	2.93	75.74	1852	-	-	303.76
SW37	1.70	1.71	567.39	1010.97	66.79	35.81	192.58	1879	-	-	46.86
SW38	3.03	0.57	544.19	1146.79	37.11	20.58	123.41	1878	-	-	76.57
SW39	5.83	3.38	1285.08	602.53	48.91	25.11	1581.20	4876	-	-	102.50
SW40	1.74	1.65	552.03	649.94	95.32	27.58	348.93	1678	-	-	53.16
SW41	4.17	1.33	646.50	1154.00	17.60	1.58	305.21	1874	-	-	299.94
SW42	6.03	1.84	611.00	1023.00	46.90	1.30	297.35	1996	-	-	215.68

"-": no data. TDS: total dissolved solids

4.1.3. Hydrodynamic Field

The water head height of No. 15 coal varies between −409.12 and 922.66 m. In the Shouyang Block, the northern and eastern parts are characterized by areas with high water potential, while the southwestern part experiences the lowest. The groundwater head height exhibits a gradual decrease from the north to south, which is closely associated with the monoclinic structure of the Shouyang Block. (Figure 4). This represents the trend of groundwater flowing from north to south [30].
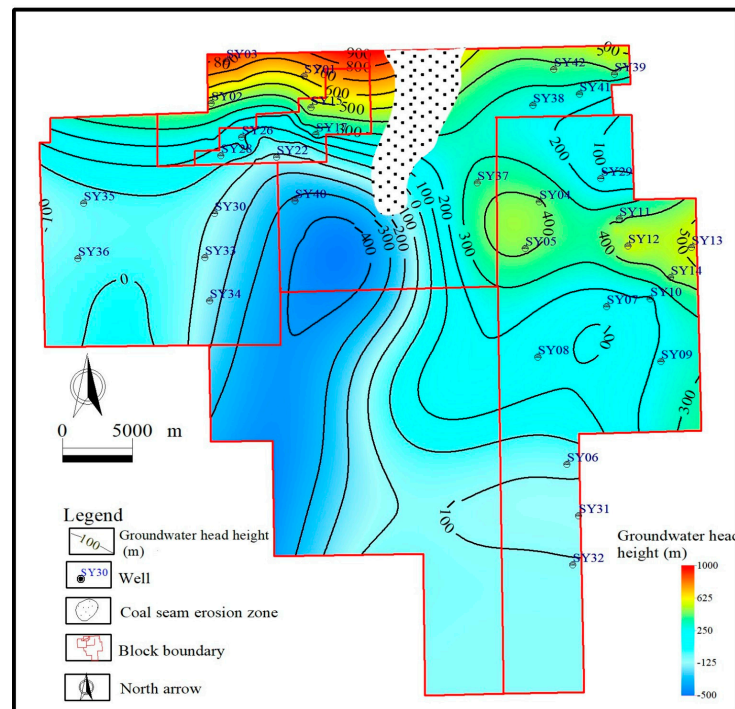
Figure 4. Isoline of water head height.

4.2. Factors Influencing Water Production

Various factors, such as the water supply, water content of the coal seam itself, fault structures, coal seam fracturing cracks, and the aquifer of the roof and floor, etc., influence the water production of coalbed methane wells [12,28]. This paper mainly conducts a comprehensive analysis of factors which include total water content of coal seams, coal seam porosity, groundwater stability index, groundwater sealing coefficient, *D* value of the fracture fractal dimension, fault fractal dimension, and sand–mud ratio.

4.2.1. Total Water Content of Coal Seam

Coal water can be classified into two categories: external water, which is easily lost in normal temperature conditions, and internal water, which is not. The total water content, a crucial parameter for evaluating its quality, is the sum of the internal and external water content of a coal sample.

Zhang Rui et al. [31] utilized acoustic logging, density logging, and neutron logging to calculate and analyze the coal composition. The calculated results exhibited a negligible absolute error in comparison to the measured results. This study collected experimental data on total water content in the study area. By integrating core positioning with logging data, an analysis of water content-sensitive parameters can be performed, and logging parameters with high correlation (AC, GR, and DEN) can be chosen. By using the laboratory's formula for calculating total water and the multiple linear regression method, a logging prediction model for total water in coal seams can be created [32]. The total water prediction model of No. 15 coal is as follow:

$$M_t = 0.012AC + 9.369DEN + 0.053GR - 18.120 \tag{2}$$

Based on the calculations of the total water content in coal seams and considering various factors such as well spacing, a prediction model for the total water content in a single-well coal seam has been established. If the well spacing in the research area is approximately 350 m, the prediction model for the total water content in a single well is as follows:

$$TCW = (350 \times 350 \times H \times DEN \times (M_t/100))/\rho_W/10000 \tag{3}$$

In the formula, *TCW* represents the total water content of coal seam, 10,000 m³; M_t represents the coal seam total water evaluation parameter, %; *H* represents the coal seam thickness, m; ρ_W represents the coal seam water density, ton/m³; *DEN* represents the density curve, ton/m³; *AC* represents the acoustic time difference, us/m³; and *GR* represents the density curve, API.

Based on the model established above, the water content of a sole well within the coal seam of the research area can be calculated. The total water content ranges from 4500 to 44,900 m³, with an average of 21,000 m³. With an increase in the total water content of the coal seam, there is a corresponding increase in the average water production (Table 3; Figure 5).
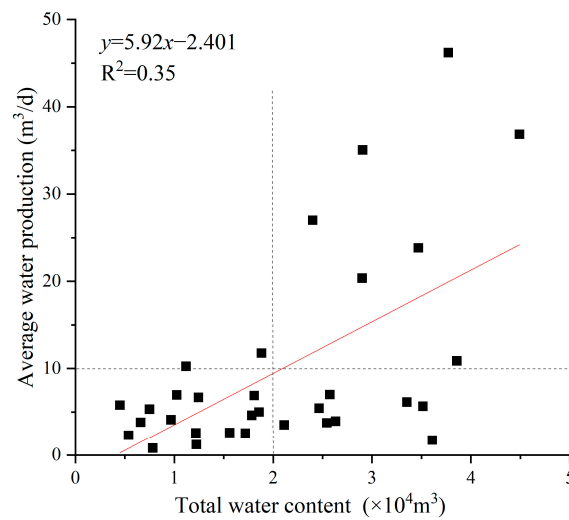
Figure 5. Relationship between average water production and total water content of coal seam.

Table 3. Data on different influencing factors.

Well	Groundwater Stability Index	D Value	Porosity (%)	Total Water Content (10,000 m³)	Fault Fractal Dimension	Sand–Mud Ratio
SY01	3.75	1.70	4.20	1.25	0.10	0.31
SY02	3.85	1.75	4.24	5.01	0.20	1.20
SY03	3.94	1.80	5.25	2.57	0.20	1.34
SY04	3.61	1.74	4.52	3.90	0.90	0.63
SY05	3.66	1.74	5.42	2.90	0.78	1.60
SY06	4.35	1.75	4.99	3.35	0.20	1.05
SY07	3.96	1.70	3.40	2.40	0.83	0.80
SY08	3.97	1.80	4.51	1.86	0.90	0.42
SY11	3.71	1.77	4.11	2.39	0.79	0.77
SY12	4.40	1.78	4.67	2.11	0.70	0.81
SY13	4.28	1.79	6.14	3.86	0.80	2.23
SY15	3.46	1.79	4.70	1.59	0.20	1.04
SY16	5.00	1.81	3.40	1.78	0.30	0.94
SY17	3.14	1.84	6.70	2.09	0.94	3.40
SY18	3.50	1.82	5.70	1.35	0.81	3.00
SY19	3.16	1.82	10.40	3.60	0.90	3.12
SY20	3.31	1.80	3.00	0.65	0.70	0.41
SY21	3.32	1.77	5.10	1.19	0.65	1.52
SY22	2.40	1.82	6.87	3.47	0.74	4.40
SY24	3.41	1.62	4.70	2.12	0.50	2.50

Table 3. *Cont.*

Well	Groundwater Stability Index	D Value	Porosity (%)	Total Water Content (10,000 m³)	Fault Fractal Dimension	Sand–Mud Ratio
SY25	3.54	1.80	5.40	1.88	0.50	3.00
SY29	3.78	1.68	4.79	1.20	0.70	0.54
SY30	3.71	1.85	4.99	5.78	0.80	2.20
SY31	4.22	1.67	3.10	1.30	0.78	0.32
SY37	3.30	1.89	6.00	0.53	0.80	1.06
SY38	3.55	1.63	4.05	0.54	0.90	0.09
SY39	3.52	1.68	3.30	1.24	0.80	2.91
SY41	3.04	1.62	6.82	0.38	0.80	1.26

4.2.2. Porosity

The characteristics of coal reservoir pores and fractures are crucial for the development of coalbed methane [33]. The greater the pore fracture space, the easier it is for water to enter the reservoir [34]. In the Shouyang Block, the porosity of coal seams varies between 2.77% and 10.4%, with an average value of 5.33%. The average water production overall increases with the increase of porosity (Figure 6).
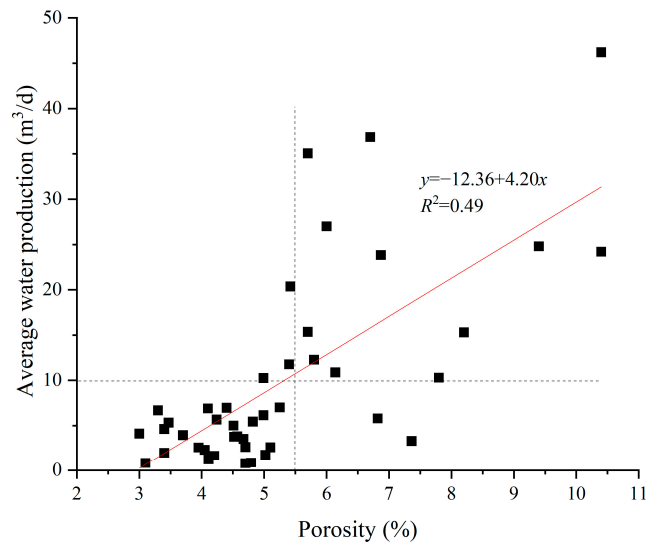
Figure 6. Relationship between average water production and porosity.

4.2.3. Groundwater Stability Index

The solubility of the groundwater medium refers to whether it has the ability to continuously dissolve soluble carbonate rocks. Currently, the commonly used method for determining this is the groundwater stability index method. The stability index of a groundwater medium can be determined by the following formula.

$$pH_s = pK_2 - pK_s - \lg[\text{ALK}] - \lg[Ca^{2+}] + p \tag{4}$$

$$p = \frac{2\sqrt{2.5 \times 10^{-5}C}}{1 + \sqrt{2.5 \times 10^{-5}C}} \tag{5}$$

$$S = pH_t - pH_s \tag{6}$$

ALK—The alkalinity of the water sample, mol/L;
PK_2—Logarithmic value of the second-order dissociation constant of carbonic acid;
PK_s—Logarithm of the dissociation constant of calcium carbonate;
Ca^{2+}—Molar concentration of calcium ions, mol/L;

C—Total dissolved solids, mg/L;

p—Correction coefficient for salt content in water;

S—Groundwater medium stability index, where pH_t is the measured value.

The solubility of a water medium worsens with increased *S*, indicating stronger precipitability and greater water medium stability [35]. A smaller stability index for a groundwater medium, on the other hand, infers greater solubility for the water medium. In the Shouyang Block, the stability index of the coal seam water medium varies between 2.94 and 4.47, with an average value of 3.63. The average water production decreases as the groundwater stability index increases, indicating that the wells with greater water production in the block are associated with the solubility of the limestone (Table 3; Figure 7).
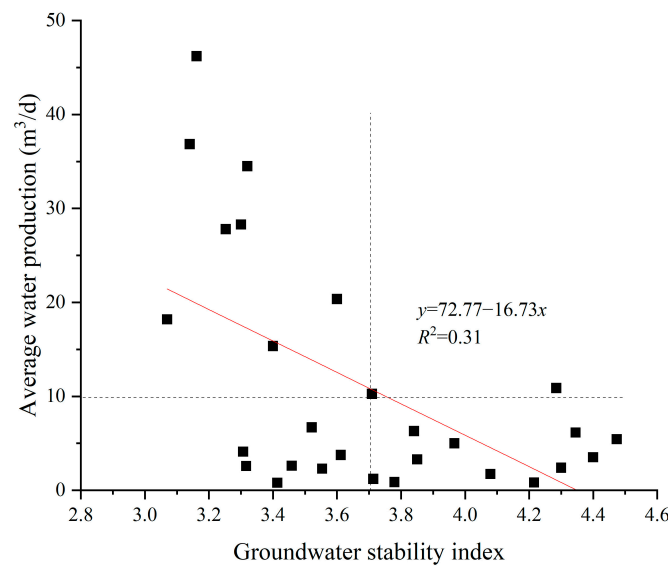
Figure 7. Relationship between average water production and groundwater stability index.

4.2.4. Groundwater Sealing Coefficient

Based on the groundwater sealing coefficient *F* proposed by previous researchers, the groundwater dynamic conditions in the study area were confirmed. The expression for the sealing coefficient is as follows:

$$F = \frac{\rho\left(K^+ + Na^+ + HCO_3^- + CO_3^{2-} + Cl^-\right)}{\rho\left(Ca^{2+} + Mg^{2+} + SO_4^{2-}\right)} \tag{7}$$

Each unit of ion concentration is given in mg/L. The sealing coefficient is constant. The larger the sealing coefficient, the better the sealing of the groundwater, which is more favourable for the enrichment and preservation of coalbed methane [36].

The groundwater sealing coefficient varies between 58.1 and 344.0, with an average of 194.6 in the study area. Approximately 65% of the coalbed methane wells exhibit a sealing coefficient exceeding 100, indicating that the groundwater in the study area has good sealing performance, poor hydrodynamic conditions, and strong groundwater retention. The average water production decreases with the increase of the sealing coefficient (Table 2; Figure 8).
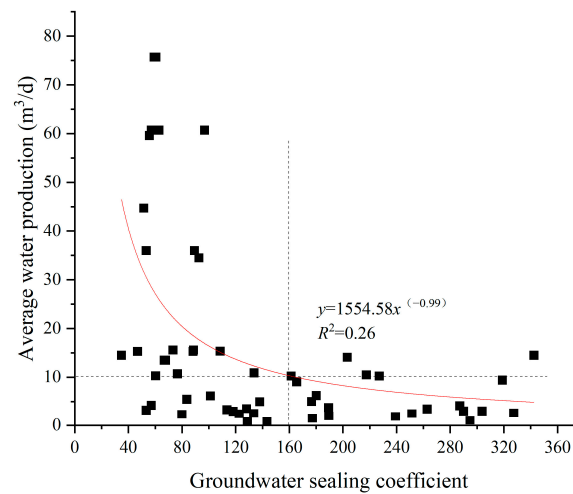
Figure 8. Relationship between average water production and sealing coefficient.

4.2.5. Fault Structure

Faults have an impact on the gas-bearing potential of coal reservoirs and fluid migration during the extraction process. The development of coalbed methane should avoid faults [37]. The closer it is to the fault, the greater the water production [38]. The fractal dimension of faults is utilized for accurately evaluation the complexity of fault structures.

The calculated results of the fractal dimension of the faults are shown in Table 3. The average water production increases with the increase in the fault fractal dimension. In simpler terms, the zones of high water yield in the study area exhibit a close correlation with the fault distribution (Figure 9).
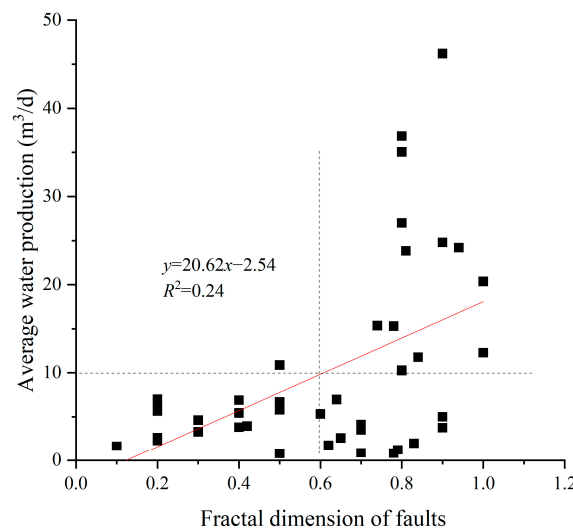
Figure 9. Relationship between average water production and fractal dimension of faults.

4.2.6. Degree of Fracture Development

Fractures are the main flow channels in coal, and the degree of coal seam fracture development can partially indicate the intensity of all tectonic processes, which could potentially affect water production [39]. The D value of the fractal dimension of fractures is an index that characterizes the degree of fracture development, mainly reflecting the size of D through the self-similarity of fractures and the anisotropy degree caused by their existence. The R/S fractal method was employed to calculate the D value. A more significant D value indicates more developed fractures.

The natural gamma fractal dimension can better evaluate the degree of fracture development. Natural gamma logging data were analyzed using the R/S fractal method to obtain the *D* value of the fracture fractal dimension that corresponds to each coalbed methane well [40,41]. The calculation results are shown in Table 3. There exists a significant positive correlation between the fractal dimension *D* value of fractures and the average water production as a whole (Figure 10).
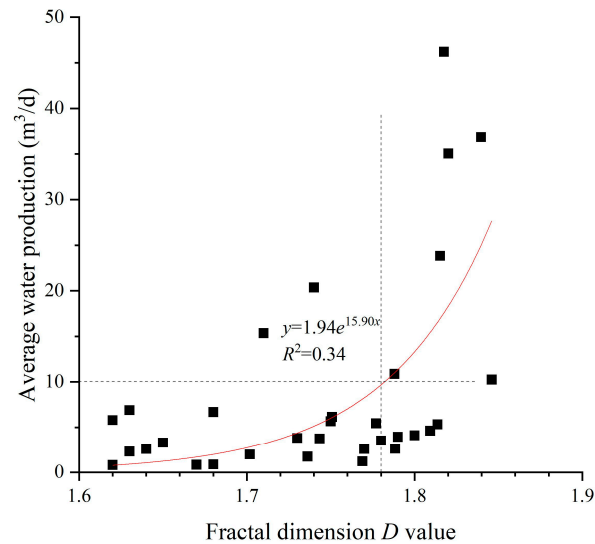

The equation shown on the plot: $y = 1.94e^{15.90x}$, $R^2 = 0.34$

Figure 10. Relationship between average water production and *D* value of fracture fractal dimension.

4.2.7. Sand–Mud Ratio

Compared to mudstone, sandstone exhibits high porosity and strong permeability [42]. The lithology determines the water content to a certain extent. Sandy mudstone and mudstone are considered as impermeable layers due to their low water content. Conversely, siltstone, fine sandstone, medium-to-coarse sandstone, and sandstone have a relatively high water content, and are regarded as aquifers. Gas production is facilitated by a greater thickness of the coal seam and mudstone, as well as a smaller thickness of the sandstone [20]. The determination was made for the sand–mud ratio between the bottom of the No. 15 coal and the K_3 limestone. The calculated results are presented in Table 3. As shown in Figure 11, there is an overall increasing trend in the average water production as the sand–mud ratio increases.
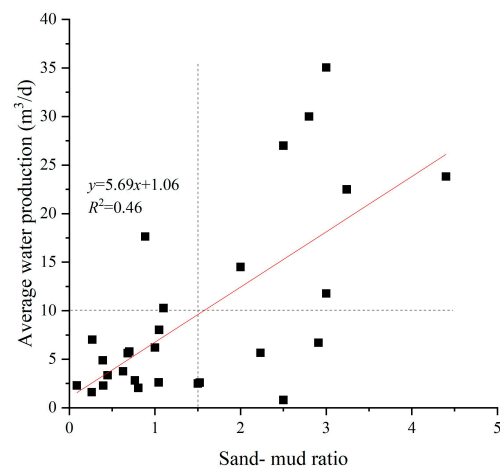

The equation shown on the plot: $y = 5.69x + 1.06$, $R^2 = 0.46$

Figure 11. Correlation of average water production with sand–mud ratio.

4.3. Analysis of the Main Influencing Factors and Classification of Water Production Types

The degree of impact of the aforementioned factors that influence the average water production of coalbed methane wells varies. Consequently, water production is a complicated variable with various levels and influencing factors. At present, due to the limitations of various objective conditions, the available data on the factors affecting average water production is very limited, belonging to a poor information system. Additionally, the existing limited data contain both known and unknown information. Therefore, the key factor influencing the average water production is a typical grey system, which can be investigated and studied through grey system theory. Important content of grey system theory is grey correlation analysis. The correlation between diverse factors within a system and its key behaviors can be quantitatively measured through grey correlation analysis, consequently identifying the primary influential factors that impact the key behaviors of the system. When two factors in a system exhibit similar changing trends, they are deemed to be strongly correlated (with a high degree of correlation). The detailed calculation process was referred to in references [37,43,44].

The correlation degree was calculated and ranked in order of magnitude (Table 4). The order of factors that influence water production, from strongest to weakest, is as follows: sand–mud ratio > porosity > fractal dimension of fault > fracture fractal dimension *D* value > groundwater sealing coefficient > groundwater stability index > total water content of coal seams.

Table 4. Correlation degree of influencing factors.

Factors Influencing Average Water Production	Sand–Mud Ratio	Porosity	Fault Fractal Dimension	Fracture Fractal Dimension *D* Value	Groundwater Sealing Coefficient	Groundwater Stability Index	Total Water Content of Coal Seams
Correlation degree	0.792	0.777	0.768	0.764	0.762	0.758	0.744

Using average water production as the classification standard, a classification of low water production was established under multi-influence factors (Table 5). The average water production is divided into low-production wells (<10 m^3/d), middle-production wells (10–20 m^3/d), and high-production wells (>20 m^3/d). When considering the values at the boundaries of each parameter, which correspond to an average water production of 10 m^3/d (as shown in Figures 6–12), certain thresholds can indicate the potential for drainage and gas production. A sand–mud ratio less than 1.5, a total water content less than 20,000 m^3, a fault fractal dimension less than 0.6, a fracture fractal dimension *D* value less than 1.78, a groundwater stability index exceeding 3.7, a porosity less than 5.5%, and a sealing coefficient greater than 160 all suggest low water production and well drainage and gas production potential.

Table 5. Classification of production well patterns for coalbed methane wells.

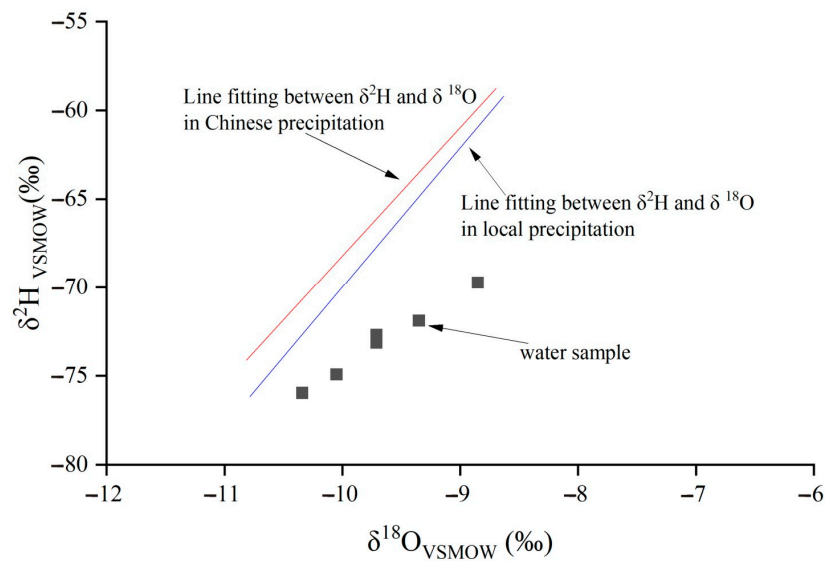| Water Production Type	Sand–Mud Ratio	Total Water Content of Coal Seams	Fault Fractal Dimension	Fracture Fractal Dimension *D* Value	Groundwater Stability Index	Porosity	Groundwater Sealing Coefficient
Low production	<1.5	<20,000 m^3	<0.6	<1.78	>3.7	<5.5%	>160
Middle production	1.5~3.5	20,000~40,000 m^3	0.6~0.8	1.78~1.82	3.2~3.7	5.5~7.5%	80~160
High production	>3.5	>40,000 m^3	>0.8	>1.82	<3.2	>7.5%	<80

Figure 12. Hydrogen and oxygen isotope characteristics of water discharged from coalbed methane wells in Shouyang Block.

4.4. Water Sources Analysis and Model of High Water Production

4.4.1. Water Sources

The Shouyang Block is generally a monoclinic structure, with unclear regional runoff and drainage zoning. The groundwater flow is not active, and the coal seam exhibits low permeability. Additionally, the coal seam itself has a low water content. Therefore, external water is the main factor affecting the difference in water production between wells [30]. The groundwater sealing coefficient, groundwater stability index, and total coal seam water content related to hydrodynamic factors and coal reservoir factors have a lower impact on water production compared to other factors.

The water discharged from coalbed methane wells in the Shouyang Block exhibits similarities with that from the Gujiao Block in the northwest of the Qinshui Basin, as well as the Shizhuang and Pan-zhuang Blocks in the southern Qinshui Basin. Due to the control of the water–rock interaction, the hydrogen and oxygen isotopes of the water discharged from coalbed methane wells are distributed near or to the right of the atmospheric precipitation line [45,46]. The isotopic composition of hydrogen and oxygen in the water sample remains consistent with the pattern of atmospheric precipitation, suggesting that the primary source of the water sample was indeed atmospheric precipitation (Figure 12) [47].

The Na^+ content in the water sample is higher than the Cl^- content, and Na^+ shows a positive correlation with Cl^-, indicating that the Na^+ and Cl^- in the water mainly come from the leaching of salt rocks, as well as other sources [48], such as the dissolution of silicate minerals (Figure 13a) [49]. When $(0.5HCO_3^{-1} + SO_4^{2-})/(Ca^{2+} + Mg^{2+}) = 1$, this indicates that the ions in groundwater mainly come from the dissolution of carbonate and sulfate rocks [50]. In the Shouyang Block, $(0.5HCO_3^{-1} + SO_4^{2-})/(Ca^{2+} + Mg^{2+})$ is much greater than 1, indicating that the dissolution amounts of carbonate and sulfate are both small (Figure 13b), and the contribution of limestone aquifers to the water production of coalbed methane wells is relatively small. Multiple sets of limestone and sandstone aquifers are developed near coal seam No. 15 in the Shouyang Block. Therefore, according to hydrochemical analysis, the water source may mainly come from the sandstone aquifer.
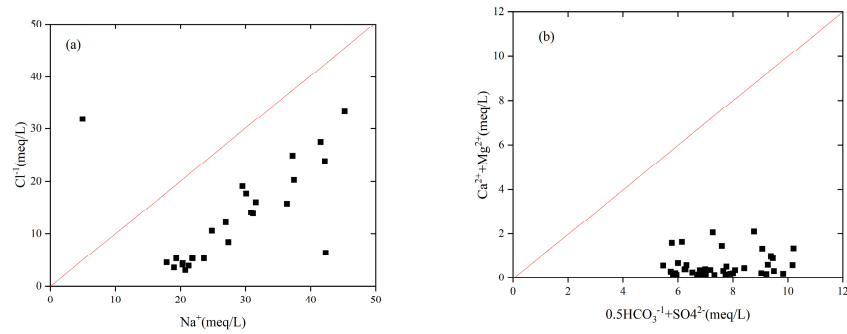
Figure 13. Diagram of ion relationships in water discharged from coalbed methane wells in Shouyang Block. (**a**) Relationship between Na^+ and Cl^- content; (**b**) Relationship between ($0.5HCO_3^{-1} + SO_4^{2-}$) and ($Ca^{2+} + Mg^{2+}$) content.

4.4.2. Model of High Water Production

The commonly used production increase measure for coalbed methane development is coal reservoir fracturing technology, and the maximum fracture length of coal rock fracturing in the Qinshui Basin can reach 20 m [51]. Further analysis of the sand–mud ratio and stratigraphic combination relationship between high-yield water wells (SY05, SY19, and SY22) and low-yield water wells (SY04, SY23, and SY38) revealed that the lithology above and below the coal seam of the low-yield water wells for single mining of No. 15 coal is mainly composed of limestone, mudstone, and sandy mudstone. Calcite thin films often appear in limestone, which are caused by later filling of cracks and, therefore, have poor water content. Although fracture structures and fracturing cracks can lead to some sandstone layers, the sandstone layers are relatively thin and have low water production (Figure 14a). The lithology above and below the coal seam of the high-yield water well for single mining of No. 15 coal is mainly composed of limestone and sandy mudstone. However, within a thickness range of 20 m, thick layers of sandstone can be seen. When fracture or fracturing cracks lead through the sandstone layer, water production increases (Figure 14b). This is similar to the high-yield water mode of natural fracture communication and fracturing fracture communication in the southern Qinshui Basin [52]. Compared with the high-yield gas areas in the southern Qinshui Basin (such as Panzhuang, Fanzhuang, and Shizhuang), the Shouyang Block has a higher permeability, stronger reservoir fluid mobility, and is more conducive to the extraction of coalbed methane. The widely distributed sand bodies with strong water supply and storage capabilities have become the main reason for high water production and low gas production [28,53]. Therefore, attention should be paid to the distribution and lithological combination of sandstone aquifers in coal-bearing strata in the future exploration and development process of the Shouyang Block. This will help to avoid the potential influence of fault structures and enable the identification of favorable areas for low water and high gas production.
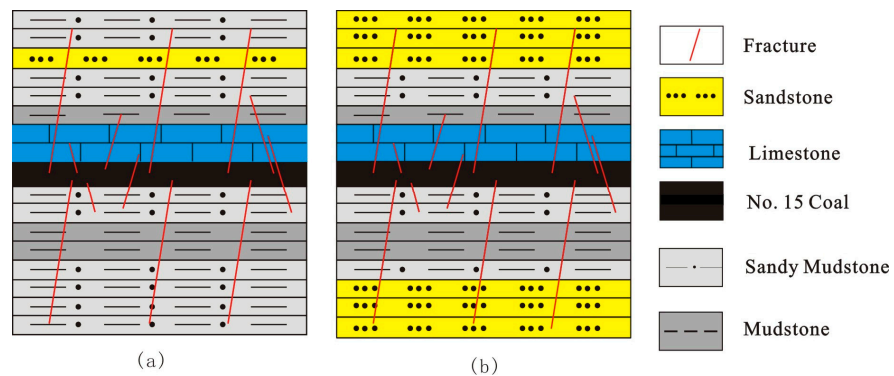

Figure 14. Water production mode of coalbed methane wells (**a**): Low water production mode in thin aquifers; (**b**): High water production mode in thick aquifers.

5. Conclusions

The groundwater head height exhibits a gradual decrease from the north to south, which represents the trend of groundwater flowing from north to south. The water dynamics in the Shouyang Block are characterized by weak groundwater runoff or retention in most areas.

The average water production ranges from 0.81 to 81.60 m^3/d. Overall, water production is relatively high. The average gas production varies between 0 and 760.57 m^3/d. Overall, the gas production is relatively low. As the average water production increases, the average gas production gradually decreases. A comprehensive analysis was conducted on the factors influencing water production, including total water content of coal seams, coal seam porosity, groundwater stability index, groundwater sealing coefficient, *D* value of the fracture fractal dimension, fault fractal dimension and sand–mud ratio.

The correlation degree was calculated and ranked in order of magnitude through grey correlation analysis. The order of factors that influence water production, from strongest to weakest, is as follows: sand–mud ratio > porosity > fractal dimension of fault > fracture fractal dimension *D* value > groundwater sealing coefficient > groundwater stability index > total water content of coal seams. The primary source of the water sample was indeed atmospheric precipitation. The dissolution amounts of carbonate and sulfate are both small, and the water source may mainly come from the sandstone aquifer. Attention should be paid to the distribution and lithological combination of sandstone aquifers in coal-bearing strata in the future exploration and development process of the Shouyang Block. Further research is needed on the hydrogeological characteristics of sandstone aquifers. This will help to avoid the potential influence of fault structures and enable the identification of favorable areas for low water and high gas production.

Author Contributions: Conceptualization, B.Z.; methodology, B.Z., G.W., W.L. and X.J.; software, G.W., W.L. and X.J.; investigation, B.Z., G.W., W.L. and X.J.; writing—original draft preparation W.L.; writing—review and editing, G.W.; project administration, B.Z.; funding acquisition, B.Z. All authors have read and agreed to the published version of the manuscript.

Institutional Review Board Statement: Not applicable.

Informed Consent Statement: Not applicable.

Data Availability Statement: The original contributions presented in the study are included in the article, further inquiries can be directed to the corresponding author.

Conflicts of Interest: Author Bing Zhang was employed by the company China United Coalbed Methane Corporation Ltd. The remaining authors declare that the research was conducted in the absence of any commercial or financial relationships that could be construed as a potential conflict of interest.

References

1. Kang, J.; Elsworth, D.; Fu, X.; Liang, S.; Chen, H. Influence of water on elastic deformation of coal and its control on per-meability in coalbed methane production. *J. Pet. Sci. Eng.* **2022**, *208*, 109603. [CrossRef]
2. Wang, L.; Sun, Y.; Zheng, S.; Shu, L.; Zhang, X. How efficient coal mine methane control can benefit carbon-neutral target: Evidence from China. *J. Clean. Prod.* **2023**, *424*, 138895. [CrossRef]
3. Sharma, R.; Singh, S.; Anand, S.; Kumar, R. A review of coal bed methane production techniques and prospects in India. *Mater. Today Proc.* **2023**, *in press*. [CrossRef]
4. Das, P.R.; Mendhe, V.A.; Kamble, A.D.; Sharma, P.; Shukla, P.; Varma, A.K. Petrographic and Geochemical Controls on Methane Genesis, Pore Fractal Attributes, and Sorption of Lower Gondwana Coal of Jharia Basin, India. *ACS Omega* **2021**, *7*, 299–324. [CrossRef] [PubMed]

5. Wei, Q.; Chen, S.; Gui, H.; Zhao, M.; Zhao, K.; Xia, H.; Wu, C. Geochemical Characteristics and Geological Significance of Coalbed Methane in Suzhou Mining Area of the Huaibei Coalfield. *ACS Omega* **2024**, *9*, 20086–20100. [CrossRef]

6. Li, Y.; Tang, D.; Xu, H.; Elsworth, D.; Meng, Y. Geological and hydrological controls on water coproduced with coalbed methane in Liulin, eastern Ordos basin, China. *AAPG Bull.* **2015**, *99*, 207–229. [CrossRef]

7. Wang, B.; Wang, D.; Cao, W.; Li, G.; Hou, W.; Cui, X.; Hou, T.; Shi, M. Review of the Hydrogeological Controls on Coalbed Methane (CBM) and Development Trends. *Geofluids* **2021**, *2021*, 8298579. [CrossRef]

8. Van, V.W.A. Geochemical signature of formation waters associated with coalbed methane. *AAPG Bull.* **2003**, *87*, 667–676.

9. Wu, J.; Guo, C.; Sang, S.; Li, G. Geochemical Characteristics of Water Produced from Coalbed Methane Wells in the Southern Qinshui Basin and Construction of an Associated Model: Implications for Coalbed Methane Co-Production. *Energies* **2022**, *15*, 8009. [CrossRef]

10. Dahm, K.G.; Guerra, K.L.; Munakata-Marr, J.; Drewes, J.E. Trends in water quality variability for coalbed methane produced water. *J. Clean. Prod.* **2014**, *84*, 840–848. [CrossRef]

11. Zhao, Z.; Liu, D.; Chen, M.; Wang, B.; Sun, J.; Yu, L.; Cai, Y.; Zhao, B.; Sun, F. Gas and water performance from the full-cycle of coalbed methane enrichment-drainage-output: A case study of Daning-jixian area in the eastern margin of Ordos Basin. *Energy Rep.* **2023**, *9*, 3235–3247. [CrossRef]

12. Du, F.F.; Ni, X.M.; Zhang, Y.F.; Wang, W.S.; Wang, K. Hydrological control mode and production characteristics of coalbed methane field in Shouyang Block. *Coal Sci. Technol.* **2023**, *51*, 177–188.

13. Du, F.; Ni, X.; Zhang, Y.; Liu, Y.; Wang, W. Recharge water types of coalbed methane wells: Controlling effects on water yield and countermeasures. *Coal Geol. Explor.* **2023**, *51*, 74–84.

14. Pashin, J.C.; McIntyre-Redden, M.R.; Mann, S.D.; Kopaska-Merkel, D.C.; Varonka, M.; Orem, W. Relationships between water and gas chemistry in mature coalbed methane reservoirs of the Black Warrior Basin. *Int. J. Coal Geol.* **2014**, *126*, 92–105. [CrossRef]

15. Huo, Z. Analysis on the Difference and Main Controlling Factors of Gas-Water Productivity of CBM Straight Wells in Zhengzhuang South Qinshui Basin. Master's Thesis, China University of Mining and Technology, Xuzhou, China, 2017.

16. Guo, C.; Qin, Y.; Wu, C.; Lu, L. Hydrogeological control and productivity modes of coalbed methane commingled pro-duction in multi-seam areas: A case study of the Bide–Santang Basin, western Guizhou, South China. *J. Pet. Sci. Eng.* **2020**, *189*, 107039. [CrossRef]

17. Yang, G.; Tang, S.; Hu, W.; Song, Z.; Zhang, S.; Xi, Z.; Wang, K.; Yan, X. Analysis of abnormally high water production in coalbed methane vertical wells: A case study of the Shizhuangnan block in the southern Qinshui Basin, China. *J. Pet. Sci. Eng.* **2020**, *190*, 107100. [CrossRef]

18. Han, J. Analysis of Influence Factors of CBM Wells in Shouyang Block. *China Coalbed Methane* **2018**, *15*, 12–16.

19. Wang, Y. Influence factors of upper water-bearing sandstone on coalbed methane well productivity—Take Shouyang Area as an example. *Petrochem. Technol.* **2022**, *29*, 170–172.

20. Zhang, B. CBM Well Produced Water Source Identification and Favorable Block Prediction in Shouyang Area. *Coal Geol. China* **2016**, *28*, 67–73.

21. Jiang, W.; Zhang, P.; Li, D.; Li, Z.; Wang, J.; Duan, Y.; Wu, J.; Liu, N. Reservoir characteristics and gas production potential of deep coalbed methane: Insights from the no. 15 coal seam in shouyang block, Qinshui Basin, China. *Unconv. Resour.* **2022**, *2*, 12–20.

22. Wang, J.; Kang, Y.; Jiang, S.; Zhang, S.; Ye, J.; Wu, J.; Zhang, B.; Guo, M. Reasons for water production difference of CBM wells in Shouyang Block, Qinshui Basin, and prediction on favorable areas. *Natur. Gas Ind.* **2016**, *36*, 52–59.

23. *HJ 776-2015*; Water quality-Determination of 32 elements-Inductively coupled plasma optical emission spectrometry. China Environmental Science Press: Beijing, China, 2015.

24. *DZ/T 0064.49-2021*; Methods for Analysis of Groundwater Quality-Part 49: Determination of Carbonate, Bicarbonate Ions, Hydroxy Titration. Ministry of Natural Resources of the People's Republic of China: Beijing, China, 2021.

25. *DZ/T 0064.50-2021*; Methods for Analysis of Groundwater Quality Part 50: Determination of Chloride Argentometric Titrimetric Method. Ministry of Natural Resources of the People's Republic of China: Beijing, China, 2021.

26. *GB/T 11899-1989*; Water Quality-Determination of Sulfate Gravimetric Method. National Bureau of Technical Supervision: Beijing, China, 1989.

27. *GB/T 37847-2019*; General Rules for Isotope Composition Analysis by Mass Spectrometry. Standards Press of China: Beijing, China, 2019.

28. Jiang, S.; Kang, Y.; Zhang, S.; Ye, J.; Zhang, B.; Wang, J.; Wu, J. Analysis on influencing factors of drainage dynamic of wells and CBM development strategy in Shizhuang block. *Nat. Gas Geosci.* **2016**, *27*, 1134–1142.

29. Wang, B.; Sun, F.; Tang, D.; Zhao, Y.; Song, Z.; Tao, Y. Hydrological control rule on coalbed methane enrichment and high yield in FZ Block of Qinshui Basin. *Fuel* **2015**, *140*, 568–577. [CrossRef]

30. Kang, Y.; Chen, J.; Zhang, B.; Zhang, S.; Wang, J. Identification of aquifers influencing the drainage of coalbed methane wells in Shouyang exploration area, Qinshui Basin. *J. China Coal Soc.* **2016**, *41*, 2263–2272.

31. Zhang, R. Evaluation Method Research on Coalbed Methane Reservoirs. Master's Thesis, Jilin University, Changchun, China, 2016.

32. Chen, X.; Wang, J.; Zhang, W.; Liu, W.; Cui, X.; Ding, A.; Ye, W.; Li, H. Water Production Forecast Method Research in Coal Seams. In Proceedings of the 2015 International Conference on Oil and Gas Field Exploration and Development, Xi'an, China, 20–21 September 2015; pp. 926–932.

33. Shen, J.; Qin, Y.; Zhao, J. Maceral contribution to pore size distribution in anthracite in the south Qinshui Basin. *Energy Fuels* **2019**, *33*, 7234–7243. [CrossRef]

34. Han, J. Linkage Evolution Mechanisms of Reservoir Water-Effective Stress-Permeability during CBM Production: A Case Study of 3# Coal Seam in Sihe Mine, Southern Qinshui Basin. Ph.D. Dissertation, China University of Mining and Technology, Xuzhou, China, 2022.

35. Zhang, X. Water Abundance Law of Ordovician and Water Inrush Forecast in Yanzhou Mine Area. Ph.D. Dissertation, China University of Mining and Technology, Xuzhou, China, 2016.

36. Wu, C.; Yang, Z.; Sun, H.; Zhang, Z.; Li, G.; Peng, H. Vertical fluid energy characteristics and orderly development suggestion in the southwest-ern region of Enhong Syncline in Yunnan. *Nat. Gas Geosci.* **2018**, *29*, 1205–1214.

37. Li, Q.; Shen, J.; Hu, H.; Ji, X. Research on the Control of CBM Well Reservoir Geological Engineering Characteristics on Productivity. *Geol. J. China Univ.* **2023**, *29*, 644–656.

38. Wang, K.; Tang, S.; Zhang, S.; Yang, N.; Xi, Z.; Zhang, Q.; Wang, J. Discussion on the causes of abnormally high water production of coalbed methane wells under the control of structural conditions and hydraulic fracturing. *J. China Coal Soc.* **2021**, *46*, 849–861.

39. Han, L.; Shen, J.; Qu, J.; Ji, C. Characteristics of a multi-scale fracture network and its contributions to flow properties in anthracite. *Energy Fuels* **2021**, *35*, 11319–11332. [CrossRef]

40. Sun, W.; Li, Y.; Fu, J.; Li, T. Review of fracture identification with well logs and seismic data. *Prog. Geophys.* **2014**, *29*, 1231–1242. (In Chinese)

41. Li, L.; Sang, X.; Chen, X. Research and progress on fracture of low-permeability reservoir. *Prog. Ceophys.* **2017**, *32*, 2472–2484. (In Chinese)

42. Li, G.; Qin, Y.; Wang, B.; Zhang, M.; Lin, Y.; Song, X.; Mi, W. Fluid seepage mechanism and permeability prediction model of multi-seam interbed coal measures. *Fuel* **2024**, *356*, 129556. [CrossRef]

43. Dang, F. Analysis of Factors Influencing the Productivity of Coalbed Methane in Different Geological Units in Shizhuangnan Block, Qinshui Basin. Master's Thesis, China University of Geosciences, Beijing, China, 2020.

44. Cao, T. Geological Control of CBM Productivity Difference in Lu'an Mining Area. Master's Thesis, China University of Mining and Technology, Xuzhou, China, 2016.

45. Fang, L.; Chen, B.; Nai, H.; Sano, Y.; Xu, S. Geochemical characteristics and source trace of coalbed methane co-produced water in Qinshui Basin. *Nat. Gas Geosci.* **2024**.

46. Zhao, C.H.; Shen, H.Y.; Wang, Z.H.; Liang, Y.P.; Zhao, Y.; Xie, H.; Tang, C.L. Hydrochemical and isotopic characteristics in the surface water of the Fenhe River basin and influence factors. *Environ. Sci.* **2022**, *43*, 4440–4448.

47. Huang, S.; Zou, J.; Han, J.; Mao, X. Application of Hydrochemical and Gray Correlation Methods in CBM Well Produced Water Source Discrimination. *Coal Geol. China* **2016**, *28*, 58–64.

48. Liu, X.; Xiang, W.; Si, B. Hydrochemical and Isotopic Characteristics in the Shallow Groundwater of the Fenhe River Basin and Indicative Significance. *Environ. Sci.* **2021**, *42*, 1739–1749.

49. Chen, Y.; Zhu, S.; Xiao, S. Discussion on controlling factors of hydrogeochemistry and hydraulic connections of groundwater in different mining districts. *Nat. Hazards* **2019**, *99*, 689–704. [CrossRef]

50. Zhai, J.; Zhang, S.; Tang, S. Hydrochemical characteristics of coalbed methane well in Yuwang bolck, Laochang, Yunnan province. *Sci. Technol. Eng.* **2021**, *21*, 5245–5254.

51. Feng, Q.; Wu, C.; Lei, B. Coal/Rock Mechanics Features of Qinshui Basin and Fracturing Crack Control. *Coal Sci. Technol.* **2011**, *39*, 100–103.

52. Zhu, X.; Liang, J.; Liu, Y.; Wang, C.; Liao, X.; Guo, G.; Lü, Y. Influencing factor and type of water production of CBM wells: Case study of Shizhuangnan block of Qinshui Basin. *Nat. Gas Geosci.* **2017**, *28*, 755–760.

53. Wang, J.; Kang, Y.; Jiang, S.; Zhang, B.; Gu, J. Difference of CBM development conditions in Shouyang and Shizhuang blocks, Qinshui basin. *Coal Geol. Explor.* **2017**, *45*, 56–62.